Beni-Suef University Journal of Basic and Applied Sciences

RESEARCH

Open Access

Characterization and potential application of microspheres from sodium alginate cross-linked with pectin from *Citrus depressa* Hayata's peels

Chien Wei-Jyun[1], Agrawal Dinesh Chandra[1], Hamdiani Saprini[1,3], Adhikari Saroj[2] and Dinar Suksmayu Saputri[1,4*]

Abstract

Background Pectin from Taiwan *Citrus depressa* Hayata's peels (CDH pectin) and sodium alginate (Na alginate) were mixed in neutral acidity to produce microhydrogel beads or microspheres. The potential use of the microspheres such as encapsulation materials for quercetin and nobiletin, DPPH (2,2-diphenyl-1-picrylhydrazyl) scavenging activity, toxic elements absorption ability, and thermal characteristics were explored.

Results Different ratios of CDH pectin and Na alginate produced microspheres of varying sizes and shapes. The highest yield (47.59%) with the broadest diameter was obtained at a Na alginate—CDH pectin ratio of 2:1, while the smallest yield was obtained from Na alginate—CDH pectin ratio of 1:3 (24.13%). Increasing the amount of Na alginate resulted in more spherical microspheres, higher heavy metals (cobalt and nickel) removal rates, yet a lower swelling ratio. A high pectin concentration also increased the encapsulation efficiency of quercetin and nobiletin, reaching 91.5% and 86.74%, respectively. Quercetin and nobiletin release analysis (in vitro) showed a slow release of drugs from the microspheres. Less than 20% quercetin and nobiletin were released from the microspheres in SGF (simulated gastric fluid) pH 1.2 solution after 2 h and more than 40% of the encapsulated drug was released in SIF (simulated intestinal fluid) pH 6.8 after 4 h. The strong DPPH scavenging activity of quercetin (99%) was not hindered by encapsulation materials. ICP-OES (inductively coupled plasma–optical emission spectrometry) analysis demonstrated that the biopolymer can absorb cobalt and nickel from water. Thermogravimetric analysis (TGA) result showed that the combination of CDH pectin and Na alginate produced a biopolymer that exhibited a weight loss of only 1.86–4.33% at 100 °C.

Conclusions These findings suggest that microspheres produced from CDH pectin cross-linked with sodium alginate had potential in nobiletin and quercetin encapsulation. Moreover, the polymer could absorb heavy metals and exhibit an important characteristic for hot food and beverage packaging applications.

Keywords Biopolymer, Pectin, Microspheres, Microencapsulation, Cross-linking

*Correspondence:
Dinar Suksmayu Saputri
dinar23ss@gmail.com
Full list of author information is available at the end of the article

1 Background

Citrus depressa Hayata (CDH) originally grew in the southwestern part of the Japanese archipelago and the mountains of Taiwan [1, 2]. Due to its sour taste, the fruit is eaten fresh, used as a garnish, or transformed into flavor enhancers, snacks, and drinks. Additionally, the juice is applied in the garment industry as a bleaching agent [3–7]. Pingtung is the main cultivation area in Taiwan, where more than 100 hectares have been planted, whereas it is also distributed in several cities and counties across Taiwan. Since 2019, the policy of the Council of Agriculture in Taiwan has urged to convert abandoned betel nut orchards into lemons, and the production area has increased from 280 to 312 hectares [8]. However, CDH food and non-food product derivatives led to a huge amount of waste, where almost 50% of the fruit mass contains approximately 40–55% peels, 30–35% pulps, and 10% seeds. Untreated citrus wastes that were directly disposed could affect the essential species in the soil and aquatic ecosystem [9–11]. Citrus wastes still contain extractable commercial bioactive compounds, including functional polysaccharides such as pectin [12, 13].

Pectin accounts for approximately 4–30% of citrus by-products, including in the endocarp and peels of CDH [6, 14–16]. Pectin is a complex hetero-polysaccharide consisting of both linear and branched mixture of sugars, which is mainly a chain of α-1,4-glycosidic poly-(D-galacturonic acid). As a biopolymer, pectin could be recovered from fruit by-products. Pectin is mostly utilized as a stabilizer or thickener in the food and pharmaceutical industry. Moreover, pectin is also a potential ingredient in the formulation of micro- and nano-capsules [17]. Different hydrophobicity of pectin plays a key role in the interaction with hydrophobic molecules. High methoxyl pectin such as CDH pectin is highly hydrophobic and has the potential to provide a controlled release profile of hydrophobic compounds such as flavonoids in the human body [18].

Flavonoids are plant secondary metabolites that are known to have antioxidant, anti-inflammatory, antiviral, anti-bacterial, and anti-carcinogenic properties. Despite these health-promoting activities, due to the unique molecule and chemical structure, flavonoids are known to be highly sensitive to environmental conditions, including light, heat, acidity, oxidation, hydrophobic, and have limited applications for health benefits because of the low bioavailability after oral intake. In this regard, several flavonoid encapsulation experiments have been conducted to preserve the stability and bioactivities and to cover unpleasant flavors at high concentrations [19–21].

Several encapsulation methods have been reported as potential approaches, where some plant polyphenols have been successfully encapsulated and utilized in the food industry [22]. Microencapsulation is an effective tool to improve the delivery of bioactive compounds, including minerals, vitamins, and antioxidants [23].

Due to the food-grade formulation and the firmness of formed capsules, the hydrogel encapsulation method has been widely exploited for food applications [24]. However, despite the single use of biopolymer as the standard hydrogel carrier, there are ongoing studies on two or more polymers to form mixed gels to improve product quality [25]. Sodium alginate (Na alginate) extracted from the cell walls of brown algae is known as a negatively charged polyelectrolyte and natural gelling agent. Under acidic conditions, the combination of sodium alginate and pectin have been reported to show strong synergy and better capsular stability. Therefore, as a result of the higher incorporation and concentration of cross-linked polymers within the matrix, the microcapsules produced were anticipated to preserve encapsulation efficiency [23].

Moreover, apart from being utilized as micro- and nano-capsules [15, 26, 27]. Pectin-alginate combination is also a potential food packaging material and toxic compound absorbent due to the ability to chelate metals [15, 17, 18]. In addition, pectin also exhibits healing properties such as preventing atherosclerosis by lowering blood cholesterol levels and high antioxidant effect by scavenging free radicals, intensifying endogenous antioxidant enzymes, and enhancing flavonoid absorption in the body [17, 27]. Potential exploration of pectin from *Citrus depressa* H. as the material for encapsulation, heavy metal adsorption, and packaging material has never been done before. Therefore, the present work aimed to initially analyze the ability of Na alginate–CDH pectin microspheres in nickel and cobalt sorption and also as microencapsulation material for quercetin and nobiletin. The combination of pectin from CDH and Na alginate is anticipated to produce microspheres that are effective for microencapsulation of bioactive compounds, exhibit significant antioxidant properties, and demonstrate efficient sorption of heavy metals such as nickel and cobalt, making them valuable for applications in food, pharmaceutical, and environmental industries.

2 Material and methods

2.1 Chemicals

Chemicals utilized in this research including acetic acid, hydrochloric acid, quercetin and analytical pectin were purchased from Sigma-Aldrich (St. Louis, MD, USA). Sodium alginate ($NaC_6H_7O_6$), sodium citrate, sodium acetate, sodium chloride (NaCl), calcium chloride anhydrous ($CaCl_2$), cobalt chloride ($CoCl_2{\cdot}6H_2O$), nickel chloride ($NiCl_2{\cdot}6H_2O$), sodium hydroxide (NaOH), and 95% ethanol were obtained from local supplier,

Choneye pure chemicals, Shimakyu's Pure Chemicals, and Echo Chemical, Taiwan. Nobiletin (purity 98%) and 2,2-diphenyl-1-picrylhydrazyl (DPPH) were purchased from Toronto Research Chemicals (Canada). Potassium phosphate monobasic was obtained from J.T Baker (Avantor Performance Materials, USA), and sodium dodecyl sulphate (SDS) was purchased from Cambridge isotope Laboratories, Inc. (USA).

2.2 Methods

2.2.1 CDH pectin extraction

The dried CDH peel powder was combined with distilled water and treated with ultrasonication according to the specified parameters. After extraction, the solids were removed from the extraction solution through centrifugation at 6000 rpm for 10 min. Pectin was precipitated by adding 98% ethanol to the solution at a 1:2 ethanol-to-solution ratio. The mixture was left to precipitate overnight at 4 °C. The precipitated pectin was then collected via centrifugation at 6000 rpm for 10 min, and the resulting pellets were dried at 40 °C [16].

2.2.2 Phenolic-pectin interaction

Spectroscopy measurements were applied to qualitatively detect the interaction between pectin and phenolic compounds (quercetin and nobiletin). The shift of UV–Vis absorbance of quercetin (Q) and nobiletin (N) in the presence of pectin was observed. Quercetin and nobiletin standards (10 mM) were added to 0.1% CDH pectin solution in acetic buffer (AB) pH 4.5 and mixed thoroughly. Hereinafter, UV–Vis absorbance in the range of 300–500 nm was recorded for a certain period (0, 4 and 24 h) [28].

2.2.3 Encapsulation of quercetin and nobiletin in Na alginate–CDH pectin microspheres

2.2.3.1 Na alginate–CDH pectin microspheres production [29] The specific amount of sodium alginate (Na alginate) and CDH pectin was dissolved in distilled water to get a 3.5% (w/v) solution with Na alginate: CDH pectin (AP) weight ratios 1:1 (AP11), 1:2 (AP12), 1:3 (AP13), 2:1 (AP21), and 3:1 (AP31). The solution then mixed thoroughly for 1 h and ultrasonicated at ambient temperature for 25 min. Uniform-size microspheres were produced by dropping the Na alginate:CDH pectin solution into 0.25 M $CaCl_2$ [30] using a 1-mL syringe and then hardened in the $CaCl_2$ solutions for 1 h. The microspheres were filtered from the solution and washed with distilled water 3–4 times to remove the remaining $CaCl_2$.

2.2.3.2 Quercetin and nobiletin-loaded microspheres production A similar microspheres production method was applied; only 2 mg of pure quercetin or nobiletin was dissolved into the freshly Na alginate solution before mixing with pectin and cross-linking by $CaCl_2$ [31].

2.2.4 Determination of sphericity coefficient (SC) of Na alginate–CDH pectin microspheres

Approximately, 10 Na alginate–CDH pectin microspheres were randomly selected for surface morphology analysis using a light microscope at 40× magnification (microscope Olympus UTV1x-2, Tokyo, Japan). The diameter of the microspheres was measured by a digital caliper. The sphericity coefficient of alginate-pectin microspheres was calculated by the following formula:

$$\mathrm{SC} = \frac{d_{\min}}{d_{\max}}$$

where $d_{\min}$ and $d_{\max}$ are the minimum and maximum Ferret's diameters of the microspheres. Microspheres with SC value close to 1 were considered ideal and spherical [25].

2.2.5 Swelling ratio

Briefly, 0.05 g microspheres were soaked in 5 mL distilled water at room temperature for 3 days. The microspheres were removed and gently tapped with filter paper to absorb any excess water. The swollen microspheres were then weighed, and the swelling ratio was determined using the following formula:

$$\text{swelling ratio}(\mathrm{g/g}) = \frac{(W_s - W_d)}{W_d}$$

where W_s is the weight of swollen microspheres and W_d is the dry weight of the microspheres [32].

2.2.6 Determination of flavonoids entrapment efficiency (EE (%)) into the microspheres

The efficiency of quercetin and nobiletin encapsulation by the microspheres was determined by UV–Vis spectra observation. Calibration curves were built by plotting the spectra of pure quercetin and nobiletin concentration series dissolved in 5% sodium citrate.

Briefly, 0.025 g of loaded microspheres was soaked in 1 mL of 5% sodium citrate ($Na_3C_6H_5O_7$) solution and stirred constantly for 6 h. Furthermore, the mixture was then centrifuged for 15 min at 12,000 rpm, and the supernatant was collected. The supernatant was then analyzed by observing the UV–Vis absorbance at 321 nm for quercetin and 334 nm for nobiletin. Entrapment efficiency was calculated using the equation:

$$\mathrm{EE}(\%) = \frac{C_{\mathrm{pQ/Ne}}}{C_{\mathrm{tQ/Ne}}} \times 100$$

where:

$C_{pQ/N\ e}$ = practical concentration of encapsulated quercetin/nobiletin, $C_{tQ/N\ e}$ = theoretical concentration of encapsulated quercetin/nobiletin.

2.2.7 Quercetin/nobiletin release (in vitro)

Simulated gastric fluid (SGF) was prepared by dissolving 3 g NaCl in 1.45 L distilled water, and then pH was adjusted to 1.2 ± 0.1 by using 0.1 M HCl. Meanwhile, simulated intestinal fluid (SIF) was prepared by dissolving 10.2 g potassium phosphate monobasic and 3.75 g SDS in 1 L distilled water, and then the pH was adjusted to 6.8 ± 0.1 by using 1 N NaOH. The volume of both fluids was adjusted to 1.5 L with distilled water [33].

For the quercetin/nobiletin release study, quercetin and nobiletin solutions in SIF pH 6.8 and SGF pH 1.2 were observed for a wide range of wavelengths, and several wavelengths were selected to calibrate the absorbances to quercetin or nobiletin concentrations (nobiletin in SGF: 334 nm; SIF: 335 nm. Quercetin in SGF: 367 nm; SIF: 369 nm). Calibration curves were built by plotting the spectra of pure quercetin and nobiletin concentration series dissolved in SGF and SIF.

Briefly, 0.03 g loaded microspheres were soaked in SGF pH 1.2 and SIF pH 6.8, incubated at 37 °C, and observed at specific time intervals (0, 2, 4, 6, 8, 10, 24 h). An aliquot from each sample was analyzed by using a UV–Vis spectrophotometer to determine the released quercetin and nobiletin [34].

2.2.8 Potentially toxic element absorption property of dried microspheres

Potentially toxic element (PTE) sorption was assessed by the method of Ju et al. [32]. Stock solutions were prepared by dissolving a certain amount of nickel and cobalt chloride in distilled water to obtain a 1 ppm concentration. Briefly, 0.03 g dried microspheres were added to nickel and cobalt stock solution and stirred constantly at ambient temperature for 24 h. The solution was separated from the microsphere and then filtered with a 0.45-µm PVDF (polyvinylidene difluoride) syringe filter. Remained nickel and cobalt concentrations were detected and measured by using Inductively Coupled Plasma–Optical Emission Spectrometry (ICP–OES - iCAP 6000, Thermo Scientific). The metal absorption capacity was calculated using the equation:

$$\text{absorption capacity}\left(\text{mg/g}\right) = (C_0 - C_e)\frac{V}{m}$$

where C_0 is the initial concentration of metals in the solution, C_e is the final (equilibrium) concentration of metals in the solution (mg L^{-1}), m (g) is the dry weight of the microspheres, and V (L) is the volume of the copper ion solution.

Metal removal rate (%) was calculated by following formula [35]:

$$\text{Removal rate}(\%) = \frac{(C_0 - C_e)}{C_0}$$

2.2.9 DPPH scavenging activity

The DPPH scavenging activity of microspheres made from CDH pectin-alginate loaded with nobiletin and quercetin was evaluated following the method of Mokhtar et al. [36]. The shift of maximum absorbance from deep violet to colorless DPPH was measured using a UV–Vis spectrometer at 517 nm. The analysis was carried out by reacting 100 µL samples with 1 mL DPPH and incubated for 30 min in the dark. DPPH scavenging activity (%) was determined by the following equation:

$$\text{DPPH scavenging activity}\ (\%) = \frac{(A_0 - A_s)}{A_0} \times 100$$

where A_0 is the absorbance of methanol (blank) and A_s is the absorbance of the sample.

2.2.10 Thermogravimetry analysis (TGA)

TGA Q-500 analyzer, Perkin-Elmer, Billerica, MA, USA, was used to determine Na alginate–CDH pectin thermal. Approximately 50 mg of dried microspheres was measured in the furnace atmosphere with the presence of nitrogen and 10 °C/min heating rate in the range of 25–600 °C [17].

2.2.11 ATR-FTIR spectroscopy analysis

Fourier transform infrared (FTIR) spectra were analyzed by Perkin-Elmer FTIR spectrometer with diamond crystal cell for attenuated total reflection (ATR) function. The spectra were collected at 4 cm^{-1} resolution with 32 scans per sample in the wavenumber range of 4000–600 cm^{-1}. The background spectrum of air was utilized to correct the spectra. Dried microsphere samples were positioned on the ATR crystal surface for measurement at room temperature. After each analysis and before collecting a spectrum from different samples, ATR crystal was cleaned thoroughly and checked spectrally.

2.2.12 Statistical analysis

Data means of three replicates were presented with standard deviation (SD), and statistical analysis was performed by SPSS for Windows version 16.0 (SPSS Inc., Chicago, IL). The differences between groups were calculated by analysis of variance (ANOVA) and Duncan's multiple comparison post-test. Statistical

significance was considered when the p value was less than 0.05 ($p < 0.05$).

3 Results

3.1 Microspheres characterization

a. Sphericity coefficient (SC)

All Na alginate-CDH pectin ratio variation (1:1, 1:2, 1:3, 2:1, 3:1) was successfully produced microspheres. Among all ratios (Table 1), the Na alginate–CDH pectin ratio 2:1 produced the highest yield (47.59%) and broadest diameter (6.8 ± 0.83 mm). Meanwhile, the lowest yield was obtained from the Na alginate–CDH pectin ratio of 1:3 (24.13%) also with the smallest diameter (3.06 ± 0.94 mm). The shape of the microspheres was observed by the sphericity coefficient (SC), which showed the ratio between the minimum and maximum Ferret's diameters of the microspheres. SC value closer to 1 signifies a more spherical shape (Fig. 1).

Table 1 Sphericity coefficient of microspheres from alginate and pectin solution

Microspheres	Sphericity coefficient (SC)
Na alginate–CDH pectin (1:1)	0.87 ± 0.05
Na alginate–CDH pectin (1:2)	0.88 ± 0.08
Na alginate–CDH pectin (1:3)	0.78 ± 0.14
Na alginate–CDH pectin (2:1)	0.89 ± 0.10
Na alginate–CDH pectin (3:1)	0.82 ± 0.13
Na alginate–CDH pectin–quercetin (1:1)	0.89 ± 0.08
Na alginate–CDH pectin–quercetin (1:2)	0.50 ± 0.18
Na alginate–CDH pectin–quercetin (1:3)	0.25 ± 0.03
Na alginate–CDH pectin–quercetin (2:1)	0.84 ± 0.11
Na alginate–CDH pectin–quercetin (3:1)	0.73 ± 0.03
Na alginate–CDH pectin–nobiletin (1:1)	0.65 ± 0.05
Na alginate–CDH pectin–nobiletin (1:2)	0.39 ± 0.11
Na alginate–CDH pectin–nobiletin (1:3)	0.48 ± 0.19
Na alginate–CDH pectin–nobiletin (2:1)	0.83 ± 0.07
Na alginate–CDH pectin–nobiletin (3:1)	0.39 ± 0.11

The results showed that more spherical microspheres, with a sphericity coefficient close to 1 (0.8–0.9), were produced with higher amounts of Na alginate. Meanwhile, more pectin and the addition of other compounds (quercetin and nobiletin) caused the decrease in SC value (0.25–0.4).

b. Swelling ratio

Hydrogel microspheres' interaction with aqueous solutions leads to swelling to a certain equilibrium that retains a significant amount of water within its structure [37]. Polyelectrolytes, alginate and pectin are prone to swelling and are sensitive to changes in acidity.

The swelling ratio was determined by recording the weight difference of the microspheres before and after they were immersed in distilled water for 3 days (Fig. 2). Compared to the study by Singh et al. [38], where the average swelling index of all citrus pectin-alginate capsule reached 0.91–0.96, the swelling index in this research is relatively low. The highest swelling value was only 0.75 in the AP12 treatment, both with or without the encapsulated material. Sasina Sai et al. [39] stated that amidated pectin does indeed swell more easily, which facilitates the prolonged release of salicylic acid at the pH level of the colon.

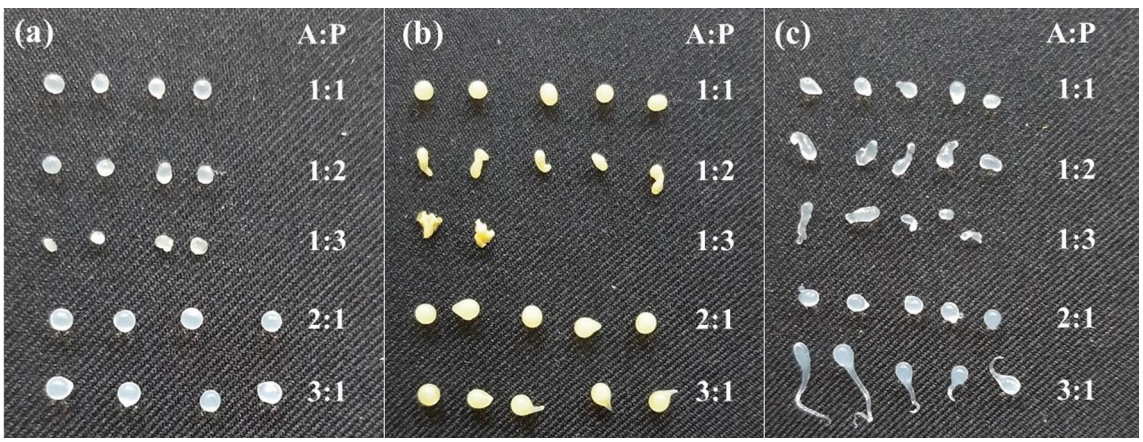

Fig. 1 CDH pectin-alginate microspheres **a** empty **b** loaded with quercetin and **c** loaded with nobiletin

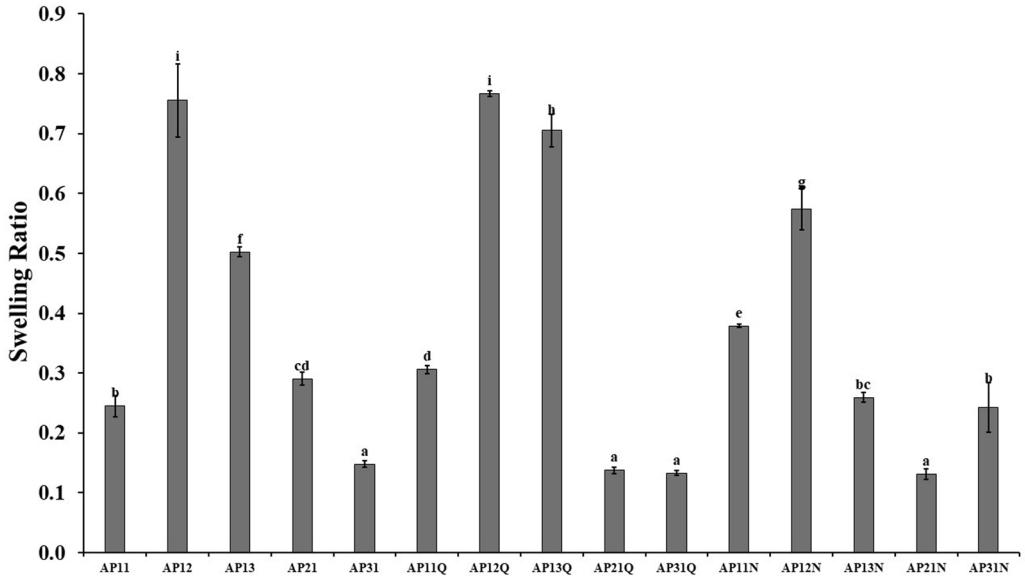

Fig. 2 The swelling ratio of Na alginate-CDH pectin (AP) with quercetin (Q) and nobiletin (N) microspheres

3.2 Potential uses of Na alginate–CDH pectin microspheres

3.2.1 Encapsulation of quercetin and nobiletin

a. Pectin-quercetin, pectin-nobiletin interaction

Spectroscopy observations were done to study the interaction between flavonoid compounds (quercetin and nobiletin) with pectin molecules in acetic buffer (AB). Quercetin and nobiletin at 10 µM final concentration were mixed with 0.1% pectin solution and incubated at room temperature for a certain period (0, 4 and 24 h). Hereinafter, the UV–Vis spectra were observed in the wavelength range 300–500 nm.

The result in Fig. 3 showed that the spectrum of pectin was shifted after quercetin and nobiletin addition. The flavonoid-pectin mixture spectrum was likely to adhere to quercetin and nobiletin. Maximum absorption of pectin was at 327 nm which shifted to 331 nm (bathochromic shift) after quercetin and nobiletin addition.

b. Flavonoid entrapment efficiency (EE (%)) into the microspheres

Quercetin and nobiletin entrapment efficiency (EE (%)) was determined by UV–Vis spectra observation. A calibration curve from the concentration series of quercetin and nobiletin in 5% sodium citrate was built. The calibration curve of quercetin is represented by the equation: $y = 0.352x + 0.1542$

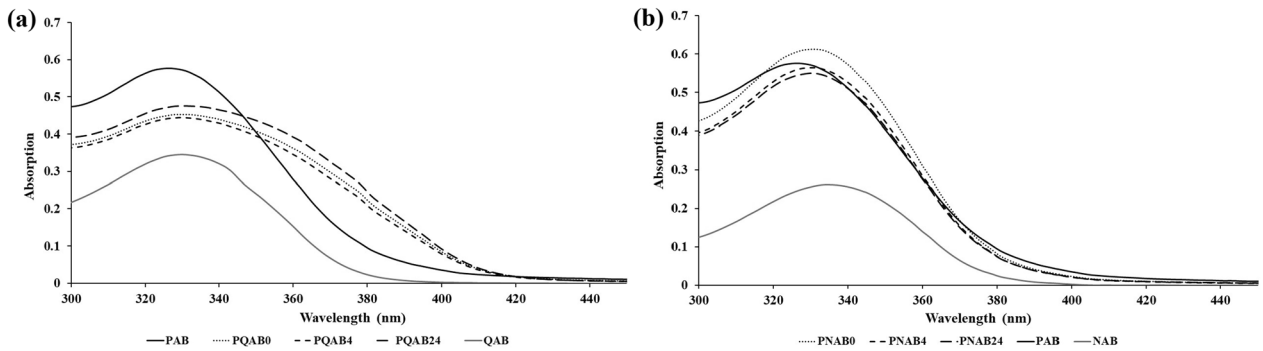

Fig. 3 Absorption spectra of **a** quercetin (Q), **b** nobiletin (N) and 0.1% (w/w) pectin (P) in acetic buffer (AB pH 4.5) at 0, 4 and 24 h. *PQ/NAB0: measurement at 0 h; PQ/NAB4: measurement at 4 h; PQ/NAB24: measurement at 24 h

with regression value 0.989; meanwhile, calibration curve of nobiletin is represented by the equation: $y=0.0438x+0.0868$ with regression value 0.977, where "*y*" refers to the absorbance of certain solutions recorded at the maximum wavelength of quercetin (321 nm) and nobiletin (334 nm) and "*x*" refers to the concentration of quercetin and nobiletin expressed as ppm. Entrapment efficiency (%) was calculated for each sample, and the results are shown in Fig. 4.

Both nobiletin and quercetin were entrapped the highest (80–90%) in Na alginate–CDH pectin ratio of 1:3 (AP13). A significant difference in EE between the alginate-pectin ratio showed that the amount of pectin affects the ability of the microsphere to preserve nobiletin and quercetin.

c. Quercetin and nobiletin release

The current method used in the research can produce Na alginate–CDH pectin microspheres containing nobiletin and quercetin, with the bioactive compounds dispersed and insoluble within the matrix (Fig. 5).

Quercetin and nobiletin pH-dependent release profile was investigated by utilizing simulated gastric fluid (SGF) pH 1.2 and simulated intestinal fluid (SIF) pH 6.8 at 37 °C (approximate body temperature). In general, the release process is driven by the solvent penetrating the hydrogel through diffusion, causing the polymer to swell, degrade, and ultimately allowing the entrapped chemicals to diffuse toward the solvent [40]. The result showed that only less than 20% quercetin and nobiletin were released from the microspheres in SGF pH 1.2 solution after 2 h (Fig. 6), whereas the microspheres significantly swelled in SIF pH 6.8, eluting more than 40% of the entrapped bioactive material after 4 h.

Na alginate–CDH pectin combination has the potential use to prolong the release pattern in SIF (pH 6.8) conditions while showing minimum release in SGF (pH 1.2).

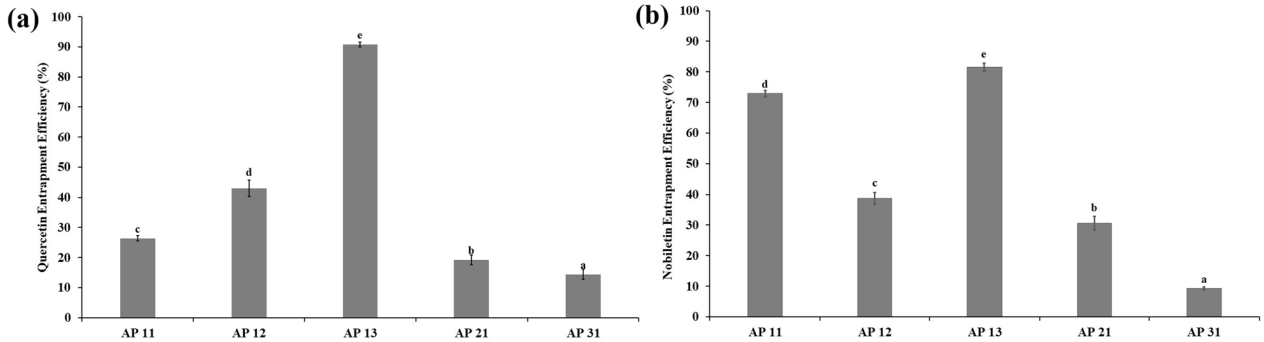

Fig. 4 Quercetin (**a**) and nobiletin (**b**) entrapment efficiency in Na alginate–CDH pectin (AP). *AP weight ratios 1:1 (AP11), 1:2 (AP12), 1:3 (AP13), 2:1 (AP21), and 3:1 (AP31)

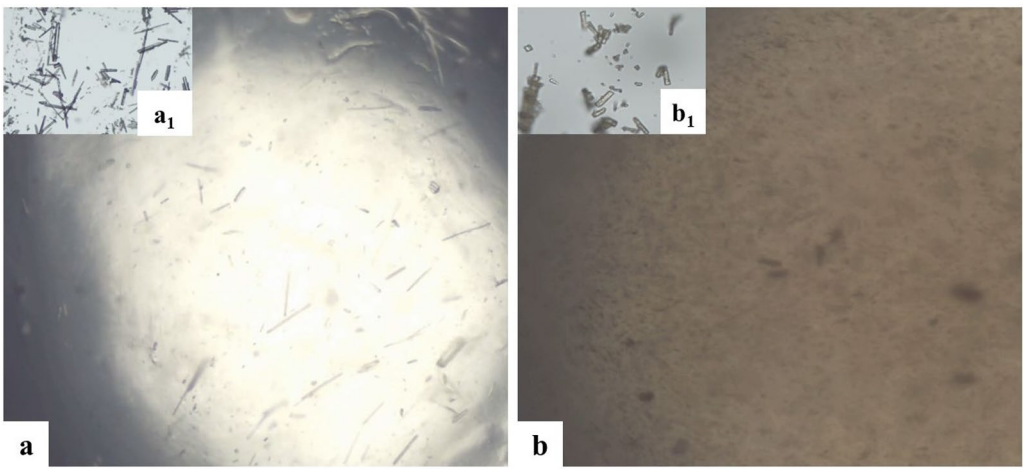

Fig. 5 Nobiletin (a_1) and quercetin (b_1) dispersed in alginate-CD pectin microspheres (a & b) Observed by light microscope at 40 × magnification

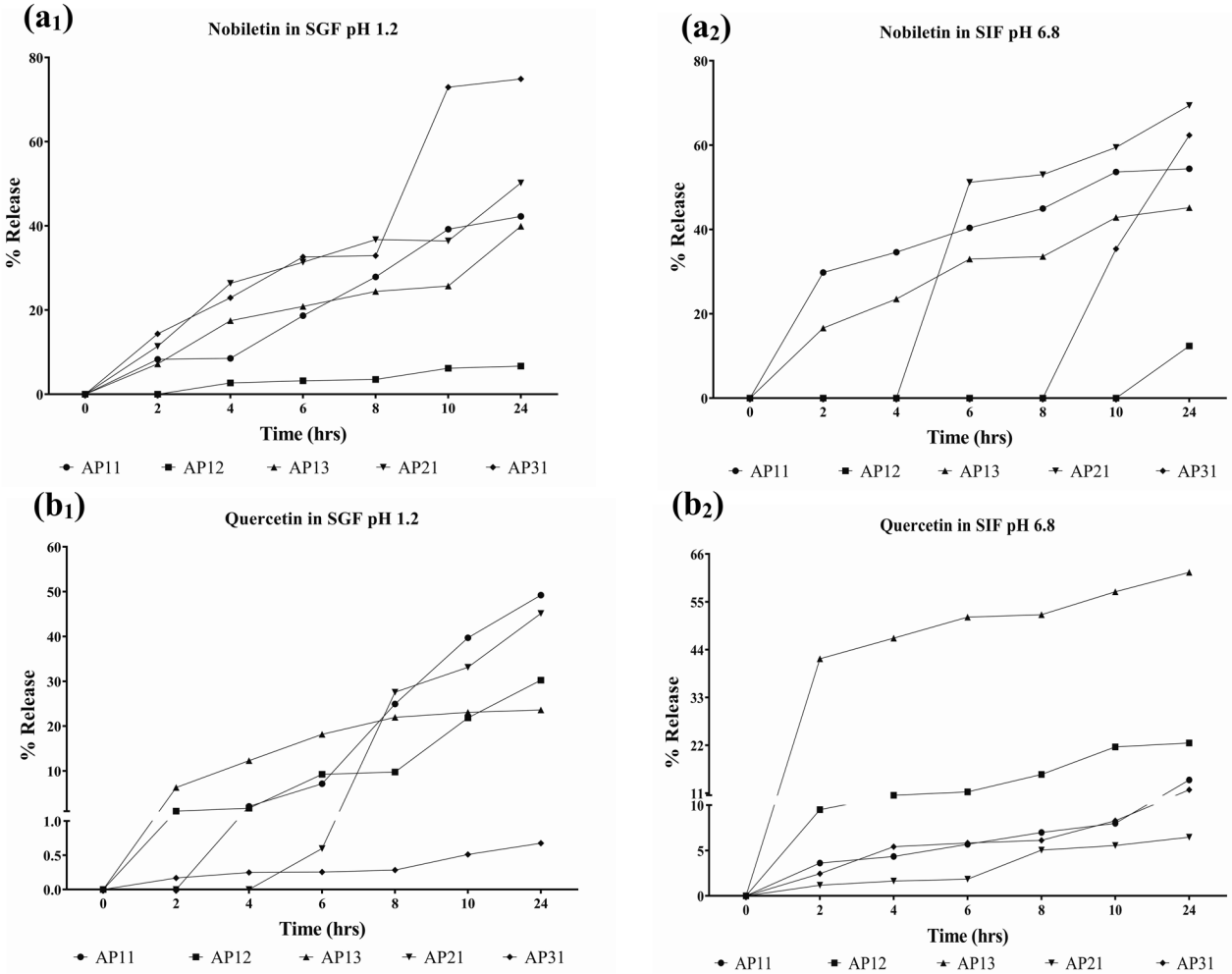

Fig. 6 Quercetin (**a**) and nobiletin (**b**) release from Na alginate–CDH pectin (AP) capsules in SGF (simulated gastric fluid) pH 1.2 (a_1 & b_1) and SIF (simulated intestinal fluid) pH 6.8 (a_2 & b_2)

d. ATR-FTIR Spectroscopy

CDH pectin, Na alginate, empty microspheres, and microspheres that contain quercetin and nobiletin were analyzed by FTIR to observe the bond between polymer and bioactive compounds (Fig. 7). Moderately intense bands absorption of CDH pectin and Na alginate was detected at around 3330 cm^{-1} related to -OH stretching vibrational modes, due to inter- and intramolecular hydrogen bonding of the galacturonic acid and the stretching vibrations of –CH bonds of methyl esters groups or pyranoid ring carbons. Weak bands between 2938 and 2830 cm^{-1} are ascribed to stretching and bending vibrations of CH, CH_2, and CH_3 bonds of methyl esters groups or pyranoid ring carbons in CDH pectin. Different from other samples where pectin was blended with Na alginate and other compounds, CDH pectin showed strong absorption at 1749 cm^{-1} which was attributed to the stretching of ester carbonyl (-$COCH_3$) groups of methyl-esterified carboxyl. Absorption bands occurring at 1602 cm^{-1} attributed to asymmetrical stretching band of carboxylate ion (COO^-), or C=O stretching vibration of the non-esterified carboxyl group of pectin. Another moderate peak at 1416 cm^{-1} is ascribed to methyl scissoring asymmetric bands of acetyls and methoxyl (–C–O–C–) groups. Strong peaks that represent polygalacturonic acid as the main polysaccharide in pectin appeared at 1227, 1088, 1023, and 833 cm^{-1}, which assigned to C=O, C–O, C–C, C–H stretching, and C-O bending. Moderate absorption peaks were found at 1360 and 800 cm^{-1}, commonly referred to as the "fingerprint" region. Specifically, when carbohydrates are the main compounds, the main stretching vibrations correspond to C–O–C and C–C bonds of the carbohydrate ring appeared in this area [41–45].

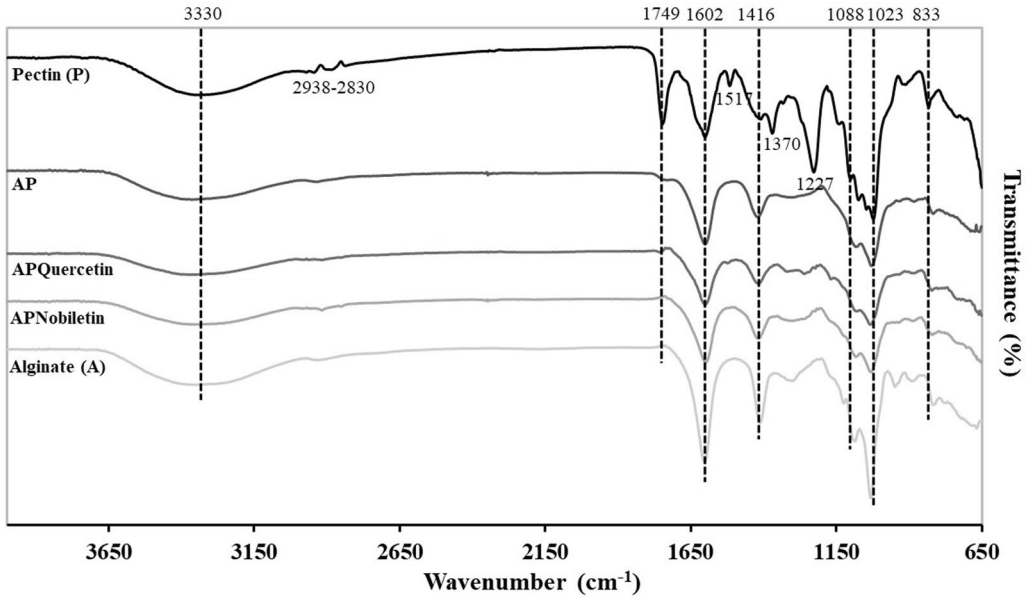

Fig. 7 FTIR spectra of Na alginate-CDH pectin microspheres

Alginate showed bands of asymmetric and symmetric stretching peaks of carboxylate salt (COO–) groups at 1602 and 1416 cm^{-1}. The band around 1027 cm^{-1} is related to C–O–C stretching, which is the characteristic of sodium alginate structure. Peaks at 1088 cm^{-1} are attributed to C–OH stretching vibrations of secondary cyclic alcohols and the band near 1023 cm^{-1} indicates a C–O–C stretching, characteristic of the sodium alginate polysaccharide structure [44, 46].

The fuse of CDH pectin with Na alginate caused the shift of -OH and asymmetric COO- stretching vibrations in CDH pectin from 3349 to 3366 cm^{-1} and from 1603 to 1600 cm^{-1}, respectively. Shifts were also detected in the fingerprint region of carbohydrates (950–1250 cm^{-1}), especially the missing spectra at 1227 cm^{-1} of the alginate-pectin, which suggests the interaction between Na alginate and CDH pectin [41, 44].

The spectral characteristic peaks of quercetin usually appeared at 3290, 1669, 1508, 1453, 1313, and 1174 cm^{-1}, which are assigned to -OH stretching, aromatic ketonic carbonyl stretching, aromatic bending, C=C stretching of the aromatic ring, OH phenolic bending, and aromatic stretching. Meanwhile, characteristic peaks of nobiletin usually exist at 1646 cm^{-1} for C=O stretching vibration as well as 1586 and 1519 cm^{-1} assigned to C=C stretching of aromatic rings [45, 47–49].

e. DPPH scavenging activity of microspheres

The result showed that the DPPH scavenging activity of entrapped quercetin is higher than empty microspheres and nobiletin microspheres. Quercetin-loaded microspheres showed high DPPH scavenging activity, whereas the sample with the highest entrapment efficiency (AP13Q) exhibited the highest DPPH scavenging activity. Meanwhile, the empty and nobiletin-loaded microspheres showed low DPPH scavenging activity (Fig. 8). Notably, the Na alginate–CDH pectin ratio microsphere with the highest nobiletin entrapment efficiency (AP13N) demonstrated the lowest DPPH scavenging activity.

3.2.2 Other potential uses of Na alginate–CDH pectin microspheres

a. Toxic element biosorbent

Agricultural waste that contains biopolymers such as pectin, chitosan, alginate, and cellulose has been studied to absorb heavy metals from aqueous suspension [50]. The present study showed the ability of Na alginate–CDH pectin microspheres to absorb nickel and cobalt (Fig. 9).

Variations in the Na alginate–CDH pectin ratio (3:1, 2:1, 1:1, 1:2, 1:3) were expected to affect the absorption capacity of cobalt and nickel. The result showed that alginate and pectin exhibit almost simi-

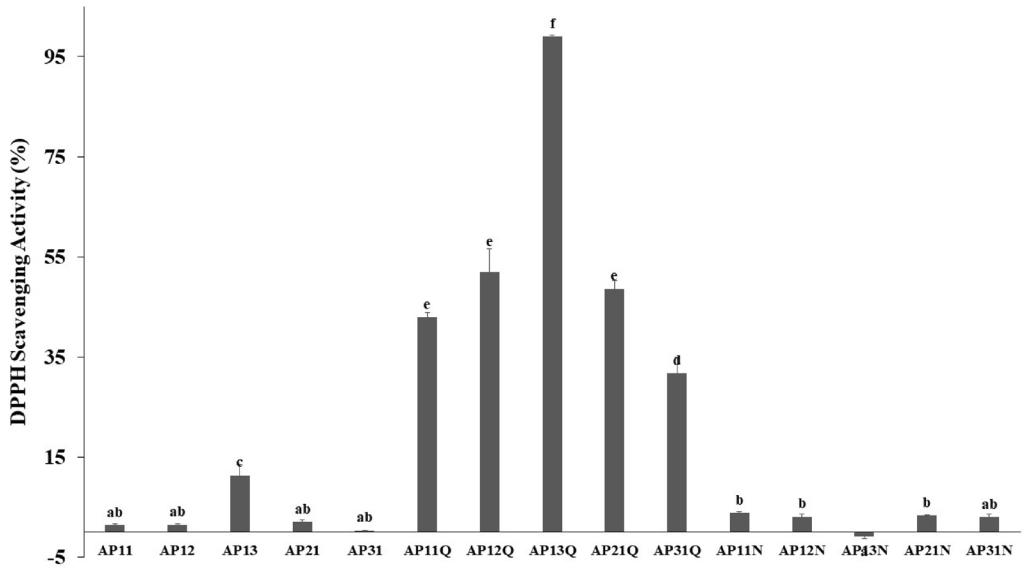

Fig. 8 DPPH scavenging activity of alginate-CDH pectin microspheres

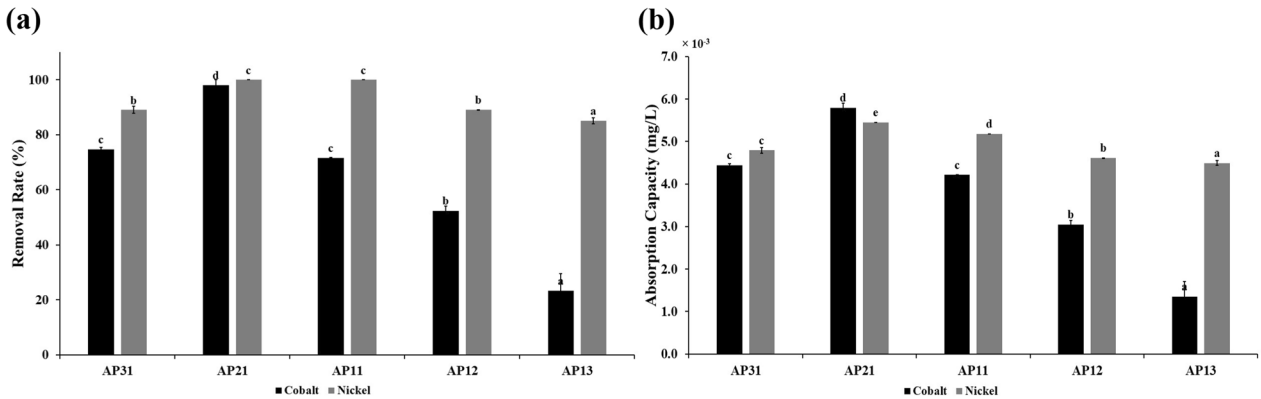

Fig. 9 Removal rate (**a**) and absorption capacity (**b**) of cobalt and nickel by Na alginate–CDH pectin (AP) microspheres for 24 h

lar effects on cobalt and nickel absorption. Excessive concentration of Na alginate or CDH pectin in the microspheres caused the decrease in removal rate. However, the best result was shown by the Na alginate–CDH pectin ratio of 2:1 with 100% absorption on both cobalt and nickel. A similar tendency was also presented in sorption capacity, where Na alginate–CDH pectin ratio 2:1 showed the highest value which is $5.79.10^{-3}$ mg metal/g microspheres for cobalt and $5.45.10^{-3}$ mg metal/g microspheres for nickel.

b. Potential use as food packaging material (based on thermal characteristics)

The thermogravimetric analysis (TGA) provides thermogram and temperature data for weight differences that represent the percentage of weight loss during the escalating temperature [17]. The thermal stability behavior of Na alginate–CDH pectin was presented in the TGA curve (Fig. 10).

The TGA curve of Na alginate–CDH pectin exhibited three stages. The first step was the mass loss between 100 and 200 °C that was associated with the loss of surface and inner moisture by evaporation or depolymerization of a pectin-alginate network [29, 46, 51]. The sharp weight loss started at 222.84 °C related to the dehydration and depolymerization of the alginate-pectin network [29, 45]. Second weight loss occurred at 276.12 °C also associated with biopolymer pyrolytic decomposition, consisting of primary and secondary decarboxylation with an acid side group and carbon in the ring [17, 52]. The final weight loss occurred at 472.19 °C, related to the formation of carbon oxide and the complete thermal degradation of the polysaccharides, which

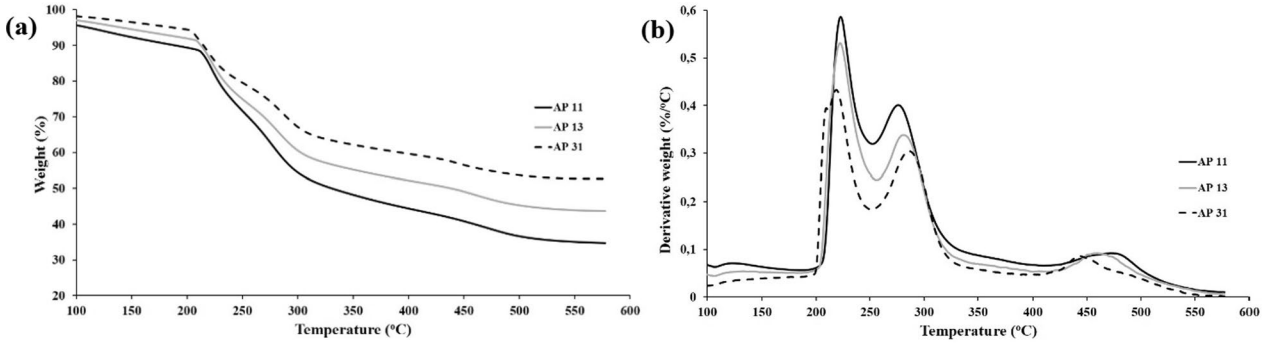

Fig. 10 Thermogravimetric (TG) (**a**) and Derivative Thermogravimetry (DTG) (**b**) profile of dried Na alginate–CDH pectin (AP) microspheres

eventually transformed into inorganic components (ashes) [29]. Higher concentrations of both pectin and alginate shifted the degradation temperature. The first sharp weight loss of microspheres with a Na alginate–CDH pectin ratio of 1:3 started at 222.42 °C, while a ratio of 3:1 started at 218.76 °C. Despite the earlier degradation temperature, the weight loss of microspheres with higher alginate or pectin was lower than the Na alginate–CDH pectin ratio 1:1 (derivative thermogravimetry - DTG curve), which means that the thermal stability is increased.

The thermogravimetric (TG) curve of Na alginate–CDH pectin 1:1 ratio microspheres showed a low amount of weight loss at 100 °C (4.33%) and lower with a higher ratio of alginate or pectin. Na alginate–CDH pectin 1:3 ratio loss of 2.94% weight, while 3:1 ratio loss of 1.86%. Moreover, 5% weight loss was achieved when the temperature reached 110.59 °C for the Na alginate–CDH pectin ratio 1:1, 141.11 °C for Na alginate–CDH pectin 1:3 and 186.9 °C for Na alginate–CDH pectin ratio 3:1.

4 Discussion

4.1 Microspheres characterization

a. Sphericity coefficient

The shape has an important role in chemical and mechanical stability. Non-spherical ones are more brittle which leads to the leaching of core ingredients before ingestion. A less viscous alginate-pectin mixture was unable to generate a spherical shape when interacting with a cross-linking solution ($CaCl_2$) [25]. Due to the controllable size and spherical shape, bead-shaped hydrogels are commonly used for absorbent applications, and bead-shaped hydrogels are more commonly used than bulk hydrogels [53]. The selection of the Na alginate–CDH pectin ratio was based on previous research by Chen and Zhang [29] on the production of aerogel microspheres for proanthocyanidin encapsulation. Experiments using ratios of 1:0, 3:1, 1:3, and 0:1 demonstrated that aerogels with a higher pectin ratio exhibited increased porosity, flexibility, water solubility, and equilibrium moisture. In contrast, aerogels with a higher alginate content exhibited more regular pore structures, greater mechanical strength, and enhanced hydrophobic properties. Ratios of 1:2 and 2:1 were added to assess the results between the 1:1 ratio, 1:3, and 3:1 ratios.

A similar study also explained that the concentration of alginate solution is a crucial factor during deformation because $CaCl_2$ might disrupt the conformation of alginate molecules when the concentration is too low. Since alginate supports an adequate strength to the membrane surrounding the microspheres, higher alginate concentration in the mixture could retain the spherical shape (Fig. 1). Microspheres' membrane with better strength could prevent the penetration of calcium chloride solution which would interrupt the sphericity of the beads [25].

The results of the current study are similar to previous research by Singh et al. [38], where capsules made with more pectin tended to take on a disk shape, and the sphericity coefficient increased with higher concentrations of sodium alginate. Both low methoxyl pectin (LMP) and high methoxyl pectins (HMP) can form gels but with distinctly different gelling conditions and mechanisms. LMP requires calcium (Ca^{2+}) ions for gel formation in a similar mechanism as alginate's "egg box" model. Meanwhile, HMP commonly requires acidic and high-sugar concentrations which generate hydrogen bonds and hydrophobic

interactions between methyl esters to form gels. The pectin used in this study is the same as used in previous research and produced using the same method. This pectin has also been structurally characterized using FTIR-ATR and NMR instruments, comparing the spectra with those of standard pectin and galacturonic acid as the main component of pectin. The comparison revealed that both pectins exhibited typical polysaccharide distribution signals. However, CDH pectin exhibited more prominent characteristic signals from the methyl and acetyl groups of the esterified galacturonic acid than standard pectin, suggesting that pectin from CDH is a high methoxyl pectin [16]. Nevertheless, previous studies also reported that the gelling speed and strength of HMP are highly affected by Ca^{2+} ions [54].

b. Swelling ratio

Swelling is one of the most essential properties of hydrogel microsphere. Hydrogels are used in various applications such as slow-release drug delivery systems, wound healing, dental implants, injectable polymers, contact lenses, and superabsorbents. Hydrogel beads' interaction with aqueous solutions leads to swelling to a certain equilibrium that retains a significant amount of water within its structure [37].

Increased interest in water-based personal care products in the market recently caused the importance of water resistance character in microspheres. The swelling ratio of Na alginate–CDH pectin microspheres decreased at the higher alginate concentration. Swelling and dissolution resistance represent water resistance properties. Previous research by Devi et al. [55] also reported similar results, where the swelling of silver nanocomposite-based sodium alginate was decreased at higher Na alginate concentrations. The low swelling ratio on microspheres containing nobiletin was probably because of the hydrophobic methoxyl content in the nobiletin. Nonetheless, the swelling ratio was not affected by the molecular weight. The high swelling ratio in the aqueous environment was attributed to the substantial presence of hydrophilic amine groups in the microspheres [32, 55]. This result suggests that pectin at proper concentration possibly had a positive effect on the swelling rate (Fig. 2).

Determination of the swelling behavior of hydrogel microspheres is a crucial evaluation parameter since the impact directly on the drug release profile and kinetics. Previous research on commercial pectin-alginate beads by Awasthi et al. [26] showed that the degree of cross-linking and pH affect swelling behavior. The dual cross-linking reaction by $CaCl_2$ and epichlorhydrin which aimed to increase the encapsulation efficiency turns out to be the cause of the decreasing swelling properties.

4.2 Potential uses of Na alginate–CDH pectin microspheres

4.2.1 Encapsulation of quercetin and nobiletin

a. Pectin-quercetin, pectin-nobiletin interaction

Spectroscopy observations were done to study the interaction between flavonoid compounds (quercetin and nobiletin) with pectin molecules. The flavonoid-pectin mixture spectrum was likely to adhere to quercetin and nobiletin. The Bathochromic shift shown in Fig. 3 indicates the increase of conjugated double bonds (π electrons) [56] which is possibly caused by the interaction of pectin with quercetin or nobiletin. A similar interaction of pectin-quercetin was also reported by Chirug et al. [28] using iron ions as a mediator and Li et al. [57] between pectin-pea protein quercetin. Wang et al. [49] stated that the obvious appearance of the nobiletin spectrum curve at its maximum wavelength showed that there was no sign of damage to nobiletin molecules after mixing with pectin.

b. Quercetin and nobiletin entrapment efficiency (EE (%)) into the microspheres

The entrapment efficiency of quercetin and nobiletin was comparable to previous research using pectin, alginate, or the combination of both as microsphere material. Sun et al. [23] demonstrated that the entrapment efficiency of tangeretin in citrus pectin-Na alginate was 71.05% and 98.92%. Meanwhile, Wang et al. [46] reported that gallic acid encapsulation efficiency by Na alginate varied in the range of 50–80% depending on the encapsulation method. Chan et al. [58] showed that the encapsulation of herbal extract by Na alginate was affected by the moisture content and swelling capability of the microsphere. The pectin-alginate combination showed less than 50% encapsulation efficiency of *Carica papaya* extract. The low value of entrapment efficiency was caused by the diffusion of polyphenols during microsphere hardening [59]. Luque-Alcaraz et al. [47] reported that chitosan nanoparticles exhibit 69.1% entrapment efficiency of nobiletin. Pectin-pea protein quercetin encapsulation was enhanced depending on the capsule material:quercetin ratio and pH of the solution [57]. Lower EE value in capsules with more alginate concentration was also reported by Pour et al. [60] in folic acid encapsulation.

Pectin is applicable as both a coating and gelling material. However, high methoxyl pectin required the presence of alginate to ensure the formation of capsules, because alginate forms an insoluble cross-link with calcium chloride ($CaCl_2$). Therefore, a pectin-alginate mixture has been reported to encapsulate several bioactive compounds including essential oils, vitamins, and proteins [23, 59]. This study shows similar results to the research by Bhattacharya et al. [40] on the encapsulation of diallyl thiosulfinate using HMP and LMP combined with sodium alginate, where the addition of pectin was found to increase encapsulation efficiency. However, it slightly differs from the findings of Singh et al. [38], who studied the encapsulation of tocopherol with HMP and observed an increase in encapsulation efficiency with higher alginate concentrations.

c. Quercetin and nobiletin release

The morphology of microparticles is distinguished into microcapsules that have a defined border between the core and the shell which provide a better encapsulation profile, and microspheres with the enclosed materials are dispersed among the network and visible at the surface. However, microspheres could protect the inner compounds, with low-investment processing, and a more simple method. Morphology affects the performance of the microparticle. Microcapsules have the potential to hold greater quantities of bioactive compounds compared to microspheres and offer a rapid release mechanism. On the other hand, microspheres with smaller amounts of core bioactive material can deliver a slower release rate, which is crucial for maintaining the bioavailability of the active compounds after ingestion [61].

Food spends 2 to 4 h in the gastric before being transferred to small intestines and spends up to 5 h to be processed through the small intestines for nutrition absorption [62, 63]. The present result is in accordance with previous research by Mukhopadhyay et al. [34] where an average of 16–27% quercetin was released in the gastric pH 1.2 after 2 h. Abundant H^+ ions in simulated gastric fluid (SGF) pH 1.2 ions could replace the Ca^{2+} ions within the hydrogel's interchain. This protonation of the carboxylic acid groups in the polymer results in the formation of insoluble alginic acid on the surface of the beads, which limits water penetration. As a result, the swelling of the beads is suspended, and the polymeric network structure remains intact [40].

However, the results showed a slow release of drugs from the microspheres, likely because the conditions did not fully replicate the intestinal environment, where digestive enzymes are present. Carboxyl groups (-COOH) on hydrogen bonds between COOH and OH groups of alginates inhibit the swelling at low pH. Nonetheless, electrostatic repulsion between the ionized acid groups (-COO-) of the polymers caused a moderate bioactive material release at SIF pH 6.8 [31, 34].

Less than 100% entrapped compound release was also reported by Maier et al. [57] where pancreatin was added in SGF as the digestive enzyme to mimic the human digestive system. The result showed that quercetin entrapped in the mixture of pectin and isolated pea protein released approximately 40–70% of SIF and SGF. Garcia-Castillo et al. [59] also reported better capsule stability of the alginate-pectin complex that caused a 30% release of gallic acid in acidic conditions, and 40–70% release at basic conditions. The encapsulated ingredient could be released after 4 h which is close to the human digestion process. This release pattern is also consistent with the findings by Bhattacharya et al. [40] and Nájera-Martínez et al. [64], who also used pectin from citrus peels combined with sodium alginate for the encapsulation of bioactive compounds from garlic [40] and gallic acid [64]. However, it differs from the study by Norcino et al. [65], which also utilized citrus peel pectin and alginate for the encapsulation of grape skin extract, where the encapsulated material was released more quickly in an acidic SGF solution.

The prolonged-release pattern of quercetin and nobiletin in simulated intestinal fluid (SIF) pH 6.8 conditions and minimum release in SGF (pH 1.2) could determine the maximum absorption of the encapsulated bioactive compounds in the small intestine (pH 6.8), minimalize the release in the gastric (pH 1.2), and avoid unabsorbed bioactive release in the large intestine [60]. Pectin is resistant to digestive enzymes such as proteases and amylases. However, pectin is degradable by intestinal microflora, which makes it applicable for colon medications, proteins, or polypeptide administration. Since pectin gels swell in aqueous media that could release a particular amount of drug compounds into the gastrointestinal tract, divalent ions including Ca^{2+}, Zn^{2+}, or other polymers such as ethylcellulose, chitosan, and hydroxypropylmethylcellulose, have been utilized to form high strength pectin gels [66].

Pectin-based microcapsules are beneficial for colon delivery but the swelling and increasing pore sizes may reduce the effectiveness of low molecular weight compounds. The hydrophilic nature of pectin limits both the quantity and distribution of hydrophobic molecules within the gel. Furthermore, phase separation between the hydrophobic cargo and the

pectin gel may undermine the hydrogel's stability and structural integrity [67].

d. ATR-FTIR Spectroscopy
The spectra of the microspheres loaded with quercetin or nobiletin were similar to those of the empty Na alginate-pectin microspheres, suggesting that there is no chemical interaction between the entrapped compounds and the microsphere materials. No chemical interaction between encapsulation materials and the bioactive compounds also occurred in previous research by Awasthi et al. [26] on the encapsulation of repaglinide using pectin-alginate, Vallejo-Castillo et al. [44] on the encapsulation of polyphenols from *Carica papaya* L. also using pectin-alginate as the encapsulation materials, Stojanovic et al. [46] on encapsulation of thyme extract, and Chan et al. [58] on encapsulation of herbal aqueous extract using Ca-alginate. This means that the entrapment process and material did not directly affect the entrapped compounds and that the bioactivity of the compounds remains unchanged.

e. DPPH scavenging activity of microspheres
Quercetin is one of the most abundant flavonoid compounds present in fruits, vegetables, and derivative products. The antioxidant activity of quercetin plays an essential role in the prevention and treatment of several diseases. Quercetin also acts as an antioxidant in the body by influencing signal transduction pathways, enzymatic activity, glutathione, and reactive oxygen species (ROS) that are caused by the environment. Quercetin exhibits strong antioxidant activity which was not hindered by encapsulation materials [68]. This result is aligned with earlier research by Sun et al. [69], where the phenolic compound carvacrol maintained its high antioxidant activity following encapsulation in a citrus pectin-alginate polymer.
Metal ions could enhance the antioxidant activity by enabling free radicals to oxidize quercetin. Therefore, quercetin interaction with metal ions resulted in high antioxidant activity. The DPPH scavenging activity of quercetin is higher compared to pure quercetin when combined with iron, copper, calcium, magnesium, ruthenium, vanadium, cobalt, cadmium, and rare earth elements [68]. This result conforms with previous research by Rizfa et al. and Sellimi et al. [70, 71]. Moreover, these results are consistent with the findings in the "*Flavonoid Entrapment Efficiency*" subsection, where AP13, which entrapped the highest amount of quercetin, exhibited the highest DPPH scavenging activity, while AP13 with the highest nobiletin entrapment showed the lowest DPPH scavenging activity. Nobiletin is a type of polymethoxyflavone that has multiple methoxy groups on its flavonoid structure. Several studies have demonstrated that an increase in polymethoxyflavone concentration can lead to the reduction of DPPH scavenging activity [72–74].

4.2.2 Other potential uses of Na alginate–CDH pectin microspheres

a. Toxic element absorbent

The increasing industrialization in the past decades has been the main reason for the pollution and decreasing water quality. One of the major environmental issues is water contamination which is caused by the release of untreated industrial wastes into the water systems. This wastewater contains highly varied heavy metal ions including copper, arsenic, lead, nickel, chromium, and cobalt. These heavy metal ions are undegradable, indecomposable, and toxic to human beings through the food chain. Biosorption is one of the applicable methods to solve this problem, due to its eco-friendliness, simplicity, lower expense, and high removal rate. Various materials have been investigated as potential biosorbents. Biopolymer hydrogels with a three-dimensional polymer network have been shown to effectively absorb dyes, heavy-metal ions, and other organic pollutants. Biopolymers such as chitosan, cellulose, pectin, and alginate are also suitable due to their high reabsorbability, adsorption capacity, biocompatibility, and versatility. Pectin and pectin-rich wastes have demonstrated a strong affinity for metal ions, making them promising candidates for biosorption. Micronization, which increases surface area, is a method used to enhance sorption capacity [50, 75–77].

Heavy metals are chemical elements which are known to be toxic at very low concentrations and have a specific gravity at least five times higher than water [78, 79]. Among several heavy metal pollutants, cobalt and nickel are considered to cause occupational and industrial health risks. Dissolving nickel from the water tanks and pipes could contaminate soft drinking water and acid beverages. Corrosion and leaching of nickel significantly contribute to more than 1 mg/day oral intake. Several sources of pollutant nickel include orthopedic implants, imitation jewellery, stainless steel kitchen utensils, and tobacco [78]. Moreover, cobalt contamination could come from mobile batteries, liquid crystal display TVs, computer monitors, cosmetic products, and several traditional medicinal practices to treat anemia and postmenopausal symp-

toms in women [79]. Furthermore, environmental pollution may be caused by mining activities [80]. However, nickel and cobalt are essential minerals that have vital roles in a wide range of biochemical, morphological, and physiological functions in the growth of plants, including seed germination and productivity. Cobalt is also known as a component of vitamin B12 where one molecule of vitamin B12 contains 4% by weight of one atom of cobalt [79, 81]. The approximate consumption of cobalt by humans is 5–40 µg/day and the tolerable limit in the soil is 0.2–0.5 ppm. Higher concentrations of threshold levels could cause toxicity to plants and humans. Nickel can cause a variety of health problems including dermatitis, cardiovascular disease, lung fibrosis, asthma, and respiratory tract cancer. Meanwhile, cobalt could generate reactive oxygen species, lipid peroxidation, alternate calcium (Ca) and iron (Fe) homeostasis, interrupt mitochondrial function, and interact with body feedback systems that would trigger erythropoiesis, induct genotoxic effects, interrupt thyroid iodine uptake, and perturbation of DNA repair processes [80–82].

Variations in Na alginate–CDH pectin ratio (3:1, 2:1, 1:1, 1:2, 1:3) were expected to affect the absorption capacity of cobalt and nickel. The result showed that alginate and pectin exhibit almost similar effects on cobalt and nickel sorption. Excessive concentration of Na alginate or CDH pectin in the microspheres caused the decrease in removal rate.

A previous study by Zhao et al. [83] also reported that alginate showed higher heavy metal-binding ability than lignin, activated charcoal, and pectin. Pectin absorbs heavy metals by forming specific binding regions which is defined as "egg box," where several free carboxyl groups from the galacturonic acid chain serve as the binding sites for the heavy metals [50]. Meanwhile, Na alginate which is seaweed biomass, contains many light metal ions such as K^+, Na^+, Ca^{2+}, Mg^{2+}, etc. that could undergo ion exchange and tend to bind stronger when in contact with solutions containing heavy metal ions [83, 84]. The sorption character was determined by the physicochemical properties of the sorbent and the effect of the external environment, including acidity and pollutants. The acidity of the solution can significantly affect the adsorption mechanism [84]. Pectin and the derivatives were analyzed to absorb heavy metals and toxic synthetic dyes from polluted areas [50, 76, 85]. Citrus pectin had a high affinity for Ni^{2+}, beet pectin for Pb^{2+} and Cu^{2+}, as well as apple pectin for Co^{2+} [50]. Meanwhile, the ability of alginate from several seaweed families was already analyzed to absorb heavy metals such as Pb^{2+}, Cu^{2+}, Cd^{2+}, Zn^{2+}, Co^{2+}, Cr^{2+}, and Ni^{2+} [83]. A case study by Koziol et al. [86] on a family living in a high uranium area who's given a pectin-alginate supplement for detoxification. The result showed that the supplement increases fecal excretion of low-level ingested heavy metal.

b. Potential use as food packaging material (based on thermal characteristics)

Several stages of polysaccharides' thermal decomposition including desorption of physically absorbed water, structural water removal (dehydration), and rupture of C–O and C–C bonds in the ring units caused the evolution of carbon monoxide, carbon dioxide, and water, followed by depolymerization, and polynuclear aromatic and graphitic carbon structures formation [46].

TGA analysis is important to observe material changes during the heating process. In this study, it was observed that this biopolymer experienced only on averaged 2% weight loss when heated above 100 °C, which is lower compared to previous research by Makaremi et al. [52] and Júnior et al. [87] on citrus pectin-alginate film cross-linked by $CaCl_2$, sodium citrate and SiO_2 which showed 7.5–20.2% weight loss at 100 °C. Moreover, 5% weight loss was achieved at 100–180 °C which is also higher than previous study of cross-linked pectin and alginate by Singh et al. [88]. These are important characters for hot food and beverage packaging applications. Apart from the potential use for microencapsulation and hot food packaging, the present study showed that dried Na alginate–CDH pectin is potentially a toxic element absorbent. An absorbent should be able to endure high temperatures, especially mining wastewater which contains several heavy metals. Research by Wang et al. [35] on pectin-based aerogels that are used to absorb Pb^{2+} showed approximately 20–40% remaining matter at 500 °C which is similar to the current result where the remaining matter was 36.59% for AP ratio 1:1, 45.34% for 1:3 AP ratio and 53.64% for AP ratio 3:1. A notable strength of this study is the use of *Citrus depressa* Hayata peel as the primary material, which is rare and therefore unique. However, this also represents a limitation of the study, as this citrus is cultivated only in East Asia, making its potential applications challenging in other countries.

5 Conclusion

This study investigated the potential use of pectin from *Citrus depressa* Hayata peels, combined with sodium alginate. The concentration ratio was used as the factor that affected the encapsulation and metal sorption ability. The result showed that more Na alginate ratio (AP21 and AP31) formed more spherical microspheres and higher cobalt and nickel absorption ability than samples with more pectin. However, a higher pectin concentration in the ratio exhibits greater efficiency in the entrapment of quercetin and nobiletin. The encapsulation of quercetin within CDH pectin and Na alginate matrix did not impair its antioxidant activity. Thermal stability analysis showed that the combination also has potential for hot food and beverage packaging material. Further research on the potential of Na alginate–CDH pectin as a bioabsorbent and biodegradable packaging material needs to be conducted.

Abbreviations

AB	Acetic buffer
AP	Na alginate–CDH pectin
C_0	Initial concentration of metals in the solution
$CaCl_2$	Calcium chloride
CDH	*Citrus depressa* Hayata
C_e	Final (equilibrium) concentration of metals in the solution
$CoCl_2{\cdot}6H_2O$	Cobalt chloride
$C_{pQ/N\,e}$	Practical concentration of encapsulated quercetin/nobiletin
$C_{tQ/N\,e}$	Theoretical concentration of encapsulated quercetin/nobiletin
d_{min}	Ferret's minimum diameter
d_{max}	Ferret's maximum diameter
DPPH	2,2-Diphenyl-1-picrylhydrazyl
EE	Entrapment efficiency
FTIR/ATR	Fourier transform infrared/attenuated total reflectance
HCl	Hydrochloric acid
HMP	High methoxyl pectins
ICP–OES	Inductively coupled plasma–optical emission spectrometry
LMP	Low methoxyl pectins
N	Nobiletin
$NaC_6H_7O_6$	Sodium alginate
$Na_3C_6H_5O_7$	Sodium citrate
NaCl	Sodium chloride
NaOH	Sodium hydroxide
$NiCl_2{\cdot}6H_2O$	Nickel chloride
PQ/NAB	Pectin-quercetin/nobiletin in acetic buffer pH 4.5
PTE	Potentially toxic element
PVDF	Polyvinylidene difluoride
Q	Quercetin
SC	Sphericity coefficient
SDS	Sodium dodecyl sulfate
SGF	Simulated gastric fluid
SIF	Simulated intestinal fluid
TGA	Thermogravimetry analysis
UV VIS	Ultraviolet–visible
W_d	Weight of dried microspheres
W_s	Weight of swollen microspheres

Acknowledgements

Authors would like to thanks to Chaoyang University of Technology for the research support

Author contributions

Chien Wei-Jyun (ORCID: 0000-0003-2618-8470) contributed to funding acquisition, supervision, resources, conceptualization, reviewing. Agrawal Dinesh Chandra (ORCID: 0000-0002-2725-7151) contributed to supervision, resources, review and editing. Hamdiani Saprini (ORCID: 0000-0003-1989-6487) contributed to data curation, methodology. Adhikari Saroj (ORCID: 0000-0002-1986-8980) contributed to data curation, methodology. Dinar Suksmayu Saputri (ORCID: 0000-0003-4213-6945) contributed to conceptualization, methodology, data curation, formal analysis, and writing-original draft. All authors read and approved the final manuscript.

Funding

This research received no specific grant from any funding agency in the public, commercial, or not-for-profit sectors.

Availability of data and material

The datasets generated and/or analyzed during the current study are not publicly available, but are available from the corresponding author on reasonable request.

Declarations

Ethics approval and consent to participate

Not applicable.

Consent for publication

Not applicable.

Competing interest

The authors declare that they hold no competing interests.

Author details

[1]Department of Applied Chemistry, Chaoyang University of Technology, 168, Jifeng E. Rd., Wufeng District, Taichung 41349, Taiwan, R.O.C.. [2]Department of Environmental Engineering and Management, Chaoyang University of Technology, Taichung, Taiwan, R.O.C.. [3]Department of Chemistry, Faculty of Mathematics and Natural Science, University of Mataram, Mataram, West Nusa Tenggara, Indonesia. [4]Present Address: Research Center for Food Technology and Processing, National Research and Innovation Agency, Gunung Kidul, Indonesia.

Received: 11 March 2024 Accepted: 15 September 2024
Published online: 29 September 2024

References

1. Ishikawa R, Badenoch N, Miyagi K, Medoruma K, Osada T, Onishi M (2016) Multi-lineages of Shiikuwasha (*Citrus depressa* Hayata) evaluated by using whole chloroplast genome sequences and its bio-diversity in Okinawa, Japan. Breed Sci 66:490–498. https://doi.org/10.1270/jsbbs.15151
2. Shiu Y-L, Lin H-L, Chi C-C, Yeh S-P, Liu C-H (2016) Effects of hirami lemon, *Citrus depressa* Hayata, leaf meal in diets on the immune response and disease resistance of juvenile barramundi, *Lates calcarifer* (bloch), against *Aeromonas hydrophila*. Fish Shellfish Immunol 55:332–338. https://doi.org/10.1016/j.fsi.2016.06.001
3. Asikin Y, Taira I, Inafuku-Teramoto S, Sumi H, Ohta H, Takara K, Wada K (2012) The composition of volatile aroma components, flavanones, and polymethoxylated flavones in Shiikuwasha (*Citrus depressa* Hayata) peels of different cultivation lines. J Agric Food Chem 60:7973–7980. https://doi.org/10.1021/jf301848s
4. Hirose N (2012) *Citrus depressa* characteristics and new application development. J Jpn Soc Food Sci Technol 59:363–368
5. Takenaka M, Nanayama K, Isobe S, Ozaki K, Miyagi K, Sumi H, Toume Y, Morine S, Ohta H (2007) Effect of extraction method on yield and quality of *Citrus depressa* juice. Food Sci Technol Res 13:281–285
6. Tamaki Y, Konishi T, Fukuta M, Tako M (2008) Isolation and structural characterisation of pectin from endocarp of *Citrus depressa*. Food Chem 107:352–361. https://doi.org/10.1016/j.foodchem.2007.08.027
7. Yamamoto M, Takakura A, Tanabe A, Teramoto S, Kita M (2017) Diversity of *Citrus depressa* Hayata (Shiikuwasha) revealed by DNA analysis. Genet Resour Crop Evol 64:805–814. https://doi.org/10.1007/s10722-016-0403-2

8. Anonymous (2021) The value-added application trend of lemongrass Potential material for functional products. Harvest Megazine
9. Das I, Arora A (2021) Kinetics and mechanistic models of solid-liquid extraction of pectin using advance green techniques- a review. Food Hydrocolloids 120:106931. https://doi.org/10.1016/j.foodhyd.2021.106931
10. Mahato N, Agarwal P, Mohapatra D, Sinha M, Dhyani A, Pathak B, Tripathi MK, Angaiah S (2021) Biotransformation of citrus waste-II: bio-sorbent materials for removal of dyes, heavy metals and toxic chemicals from polluted water. Processes 9:1544. https://doi.org/10.3390/pr9091544
11. Mahato N, Sinha M, Sharma K, Koteswararao R, Cho MH (2019) Modern extraction and purification techniques for obtaining high purity food-grade bioactive compounds and value-added co-products from citrus wastes. Foods 8:523. https://doi.org/10.3390/foods8110523
12. Gómez-Mejía E, Rosales-Conrado N, León-González ME, Madrid Y (2019) Citrus peels waste as a source of value-added compounds: extraction and quantification of bioactive polyphenols. Food Chem 295:289–299. https://doi.org/10.1016/j.foodchem.2019.05.136
13. Diniso T, Oriola AO, Adeyemi JO, Miya GM, Hosu YS, Oyedeji OO, Kuria SK, Oyedeji AO (2024) Citrus wastes: a valuable raw material for biological applications. J Appl Pharm Sci. https://doi.org/10.7324/JAPS.2024.158781
14. Guo X, Zhao W, Liao X, Hu X, Wu J, Wang X (2017) Extraction of pectin from the peels of pomelo by high-speed shearing homogenization and its characteristics. LWT Food Sci Technol 79:640–646. https://doi.org/10.1016/j.lwt.2016.12.001
15. Picot-Allain MCN, Ramasawmy B, Emmambux MN (2022) Extraction, characterisation, and application of pectin from tropical and sub-tropical fruits: a review. Food Rev Intl 38:282–312. https://doi.org/10.1080/87559129.2020.1733008
16. Chien W-J, Saputri DS, Yanti S, Agrawal DC (2022) Response surface methodology for simple non-acid ultrasonic-assisted extraction of pectin from Taiwan's *Citrus depressa* H. Peels. CMUJNS. https://doi.org/10.12982/CMUJNS.2022.062
17. Kozioł A, Środa-Pomianek K, Górniak A, Wikiera A, Cyprych K, Malik M (2022) Structural determination of pectins by spectroscopy methods. Coatings 12:546. https://doi.org/10.3390/coatings12040546
18. Rehman A, Ahmad T, Aadil RM, Spotti MJ, Bakry AM, Khan IM, Zhao L, Riaz T, Tong Q (2019) Pectin polymers as wall materials for the nano-encapsulation of bioactive compounds. Trends Food Sci Technol 90:35–46. https://doi.org/10.1016/j.tifs.2019.05.015
19. Milea Ștefania A, Vasile MA, Crăciunescu O, Prelipcean A-M, Bahrim GE, Râpeanu G, Oancea A, Stănciuc N (2020) Co-microencapsulation of flavonoids from yellow onion skins and lactic acid bacteria lead to multifunctional ingredient for nutraceutical and pharmaceutics applications. Pharmaceutics 12:1053. https://doi.org/10.3390/pharmaceutics12111053
20. Yousefi M, Shadnoush M, Sohrabvandi S, Khorshidian N, M. Mortazavian A, (2021) Encapsulation systems for delivery of flavonoids: a review. Biointerface Res Appl Chem 11:13934–13951. https://doi.org/10.33263/BRIAC116.1393413951
21. Roy A, Khan A, Ahmad I, Alghamdi S, Rajab BS, Babalghith AO, Alshahrani MY, Islam S, Islam MdR (2022) Flavonoids a bioactive compound from medicinal plants and its therapeutic applications. Biomed Res Int 2022:1–9. https://doi.org/10.1155/2022/5445291
22. Vonghirundecha P, Chusri S, Meunprasertdee P, Kaewmanee T (2022) Microencapsulated functional ingredients from a *Moringa oleifera* leaf polyphenol-rich extract: characterization, antioxidant properties, in vitro simulated digestion, and storage stability. LWT 154:112820. https://doi.org/10.1016/j.lwt.2021.112820
23. Sun X, Cameron RG, Manthey JA, Hunter WB, Bai J (2020) Microencapsulation of tangeretin in a citrus pectin mixture matrix. Foods 9:1200. https://doi.org/10.3390/foods9091200
24. Molino S, Rufián Henares JÁ, G. Gómez-Mascaraque L, (2022) Impact of gelatine coating on the performance of tannin-loaded pectin microbeads obtained through external gelation. Food Struct 32:100256. https://doi.org/10.1016/j.foostr.2022.100256
25. Azhar MF, Haris MS, Mohamad I, Ismadi MNS, Yazid AAH, Rahman SR, Azlan NH (2021) Optimisation of alginate-pectin bead formulation using central composite design guided electrospray technique. Int Food Res J 28:860–870. https://doi.org/10.47863/ifrj.28.4.22
26. Awasthi R, Kulkarni GT, Ramana MV, Pinto TDJA, Kikuchi IS, Ghisleni DDM, De Souza Braga M, De Bank P, Dua K (2017) Dual crosslinked pectin–alginate network as sustained release hydrophilic matrix for repaglinide. Int J Biol Macromol 97:721–732. https://doi.org/10.1016/j.ijbiomac.2017.01.050
27. Huang X, Li T, Li S (2023) Encapsulation of vitexin-rhamnoside based on zein/pectin nanoparticles improved its stability and bioavailability. Curr Res Food Sci 6:100419. https://doi.org/10.1016/j.crfs.2022.100419
28. Chirug L, Okun Z, Ramon O, Shpigelman A (2018) Iron ions as mediators in pectin-flavonols interactions. Food Hydrocoll 84:441–449. https://doi.org/10.1016/j.foodhyd.2018.06.039
29. Chen K, Zhang H (2019) Alginate/pectin aerogel microspheres for controlled release of proanthocyanidins. Int J Biol Macromol 136:936–943. https://doi.org/10.1016/j.ijbiomac.2019.06.138
30. Cheewatanakornkool K, Sriamornsak P (2014) Pectin-chitosan multilayer coated microbeads of diclofenac sodium prepared by layer-by-layer technique. AMR 1060:45–49. https://doi.org/10.4028/www.scientific.net/AMR.1060.45
31. Frenț OD, Duteanu N, Teusdea AC, Ciocan S, Vicaș L, Jurca T, Muresan M, Pallag A, Ianasi P, Marian E (2022) Preparation and characterization of chitosan-alginate microspheres loaded with quercetin. Polymers 14:490. https://doi.org/10.3390/polym14030490
32. Ju S, Shin G, Lee M, Koo JM, Jeon H, Ok YS, Hwang DS, Hwang SY, Oh DX, Park J (2021) Biodegradable chito-beads replacing non-biodegradable microplastics for cosmetics. Green Chem 23:6953–6965. https://doi.org/10.1039/D1GC01588E
33. Pan X, Li J, Gan R, Hu X (2015) Preparation and in vitro evaluation of enteric-coated tablets of rosiglitazone sodium. Saudi Pharm J 23:581–586. https://doi.org/10.1016/j.jsps.2015.02.018
34. Mukhopadhyay P, Maity S, Mandal S, Chakraborti AS, Prajapati AK, Kundu PP (2018) Preparation, characterization and in vivo evaluation of pH sensitive, safe quercetin-succinylated chitosan-alginate core-shell-corona nanoparticle for diabetes treatment. Carbohyd Polym 182:42–51. https://doi.org/10.1016/j.carbpol.2017.10.098
35. Wang R, Li Y, Shuai X, Chen J, Liang R, Liu C (2021) Development of pectin-based aerogels with several excellent properties for the adsorption of Pb^{2+}. Foods 10:3127. https://doi.org/10.3390/foods10123127
36. Mokhtar M, Bouamar S, Di Lorenzo A, Temporini C, Daglia M, Riazi A (2021) The influence of ripeness on the phenolic content, antioxidant and antimicrobial activities of pumpkins (*Cucurbita moschata* Duchesne). Molecules 26:3623. https://doi.org/10.3390/molecules26123623
37. Shivakumara LR, Demappa T (2019) Synthesis and swelling behavior of sodium alginate/poly(vinyl alcohol) hydrogels. TJPS 16:252–260. https://doi.org/10.4274/tjps.galenos.2018.92408
38. Singh J, Kaur K, Kumar P (2018) Optimizing microencapsulation of α-tocopherol with pectin and sodium alginate. J Food Sci Technol 55:3625–3631. https://doi.org/10.1007/s13197-018-3288-6
39. Sai OKS, Aravind UK, Aravindakumar CT (2024) Pectin-based encapsulation systems for bioactive components. In: Biomaterials in Microencapsulation [Working Title]. IntechOpen
40. Bhattacharya S, Das S, Banik S (2024) Fabrication and physicochemical investigation of pH-responsive alginate/pectin hybrid network hydrogel for improved stability and controlled release of diallyl thiosulfinate. Mater Today Commun 38:108235. https://doi.org/10.1016/j.mtcomm.2024.108235
41. Nešić A, Onjia A, Davidović S, Dimitrijević S, Errico ME, Santagata G, Malinconico M (2017) Design of pectin-sodium alginate based films for potential healthcare application: study of chemico-physical interactions between the components of films and assessment of their antimicrobial activity. Carbohyd Polym 157:981–990. https://doi.org/10.1016/j.carbpol.2016.10.054
42. Pereira PHF, Oliveira TÍS, Rosa MF, Cavalcante FL, Moates GK, Wellner N, Waldron KW, Azeredo HMC (2016) Pectin extraction from pomegranate peels with citric acid. Int J Biol Macromol 88:373–379. https://doi.org/10.1016/j.ijbiomac.2016.03.074
43. Rodsamran P, Sothornvit R (2019) Extraction of phenolic compounds from lime peel waste using ultrasonic-assisted and microwave-assisted extractions. Food Biosci 28:66–73. https://doi.org/10.1016/j.fbio.2019.01.017
44. Vallejo-Castillo V, Rodríguez-Stouvenel A, Martínez R, Bernal C (2020) Development of alginate-pectin microcapsules by the extrusion for encapsulation and controlled release of polyphenols from papaya (*Carica papaya* L.). J Food Biochem. https://doi.org/10.1111/jfbc.13331

45. Wang X, Xie H, Shi C, Dziugan P, Zhao H, Zhang B (2021) Fabrication and characterization of gel beads of whey isolate protein-pectin complex for loading quercetin and their digestion release. Gels 8:18. https://doi.org/10.3390/gels8010018
46. Stojanovic R, Belscak-Cvitanovic A, Manojlovic V, Komes D, Nedovic V, Bugarski B (2012) Encapsulation of thyme (*Thymus serpyllum* L.) aqueous extract in calcium alginate beads. J Sci Food Agric 92:685–696. https://doi.org/10.1002/jsfa.4632
47. Luque-Alcaraz AG, Lizardi J, Goycoolea FM, Valdez MA, Acosta AL, Iloki-Assanga SB, Higuera-Ciapara I, Argüelles-Monal W (2012) Characterization and antiproliferative activity of nobiletin-loaded chitosan nanoparticles. J Nanomater 2012:1–7. https://doi.org/10.1155/2012/265161
48. Manthey JA (2006) Fourier transform infrared spectroscopic analysis of the polymethoxylated flavone content of orange oil residues. J Agric Food Chem 54:3215–3218. https://doi.org/10.1021/jf053134a
49. Wang X, Zhou B, Wu D, Chen X, Li B, Wang L, Liang H (2022) Ultrasound-based one-step fabrication of nobiletin particle: a facile stabilization strategy. Food Chem 369:130896. https://doi.org/10.1016/j.foodchem.2021.130896
50. Wang R, Liang R, Dai T, Chen J, Shuai X, Liu C (2019) Pectin-based adsorbents for heavy metal ions: a review. Trends Food Sci Technol 91:319–329. https://doi.org/10.1016/j.tifs.2019.07.033
51. Kumar M, Mishra RK, Banthia AK (2010) Development of pectin based hydrogel membranes for biomedical applications. Int J Plast Technol 14:213. https://doi.org/10.1007/s12588-011-0019-5
52. Makaremi M, Yousefi H, Cavallaro G, Lazzara G, Goh CBS, Lee SM, Solouk A, Pasbakhsh P (2019) Safely dissolvable and healable active packaging films based on alginate and pectin. Polymers 11:1594. https://doi.org/10.3390/polym11101594
53. Shao Z, Huang X, Yang F, Zhao W, Zhou X, Zhao C (2018) Engineering sodium alginate-based cross-linked beads with high removal ability of toxic metal ions and cationic dyes. Carbohyd Polym 187:85–93. https://doi.org/10.1016/j.carbpol.2018.01.092
54. Yang Y, Zhang G, Hong Y, Gu Z, Fang F (2013) Calcium cation triggers and accelerates the gelation of high methoxy pectin. Food Hydrocoll 32:228–234. https://doi.org/10.1016/j.foodhyd.2013.01.003
55. Karthiga Devi G, Senthil Kumar P, Sathish Kumar K (2016) Green synthesis of novel silver nanocomposite hydrogel based on sodium alginate as an efficient biosorbent for the dye wastewater treatment: prediction of isotherm and kinetic parameters. Desalin Water Treat. https://doi.org/10.1080/19443994.2016.1178178
56. Meier H, Gerold J, Kolshorn H, Mühling B (2004) Extension of conjugation leading to bathochromic or hypsochromic effects in OPV series. Chem Eur J 10:360–370. https://doi.org/10.1002/chem.200305447
57. Li J, Zhang X, Zhao R, Lu Y, Wang C, Wang C (2022) Encapsulation of quercetin in pea protein-high methoxyl pectin nanocomplexes: formation, stability, antioxidant capacity and in vitro release profile. Food Biosci 48:101811. https://doi.org/10.1016/j.fbio.2022.101811
58. Chan E-S, Yim Z-H, Phan S-H, Mansa RF, Ravindra P (2010) Encapsulation of herbal aqueous extract through absorption with ca-alginate hydrogel beads. Food Bioprod Process 88:195–201. https://doi.org/10.1016/j.fbp.2009.09.005
59. Garcia-Castillo V, Komatsu R, Clua P, Indo Y, Takagi M, Salva S, Islam MdA, Alvarez S, Takahashi H, Garcia-Cancino A, Kitazawa H, Villena J (2019) Evaluation of the immunomodulatory activities of the probiotic strain *Lactobacillus fermentum* UCO-979C. Front Immunol 10:1376. https://doi.org/10.3389/fimmu.2019.01376
60. Kiaei Pour P, Alemzadeh I, Vaziri AS, Beiroti A (2020) Potential effects of alginate–pectin biocomposite on the release of folic acid and their physicochemical characteristics. J Food Sci Technol 57:3363–3370. https://doi.org/10.1007/s13197-020-04369-7
61. Arenas-Jal M, Suñé-Negre JM, García-Montoya E (2020) An overview of microencapsulation in the food industry: opportunities, challenges, and innovations. Eur Food Res Technol 246:1371–1382. https://doi.org/10.1007/s00217-020-03496-x
62. Fish EM, Burns B (2022) Physiology, small bowel. In: StatPearls. StatPearls Publishing, Treasure Island (FL)
63. Pathikonda M, Sachdeva P, Malhotra N, Fisher RS, Maurer AH, Parkman HP (2012) Gastric emptying scintigraphy: is four hours necessary? J Clin Gastroenterol 46:209–215. https://doi.org/10.1097/MCG.0b013e31822f3ad2
64. Nájera-Martínez EF, Flores-Contreras EA, Araújo RG, Iñiguez-Moreno M, Sosa-Hernández JE, Iqbal HMN, Pastrana LM, Melchor-Martínez EM, Parra-Saldívar R (2023) Microencapsulation of gallic acid based on a polymeric and pH-sensitive matrix of pectin/alginate. Polymers 15:3014. https://doi.org/10.3390/polym15143014
65. Norcino LB, Mendes JF, Figueiredo JDA, Oliveira NL, Botrel DA, Mattoso LHC (2022) Development of alginate/pectin microcapsules by a dual process combining emulsification and ultrasonic gelation for encapsulation and controlled release of anthocyanins from grapes (*Vitis labrusca* L.). Food Chem 391:133256. https://doi.org/10.1016/j.foodchem.2022.133256
66. Martău GA, Mihai M, Vodnar DC (2019) The use of chitosan, alginate, and pectin in the biomedical and food sector—biocompatibility, bioadhesiveness, and biodegradability. Polymers 11:1837. https://doi.org/10.3390/polym11111837
67. Morales-Medina R, Drusch S, Acevedo F, Castro-Alvarez A, Benie A, Poncelet D, Dragosavac MM, Defain Tesoriero MV, Löwenstein P, Yonaha V, Iturralde R, Gauna Peter R, De Vos P (2022) Structure, controlled release mechanisms and health benefits of pectins as an encapsulation material for bioactive food components. Food Funct 13:10870–10881. https://doi.org/10.1039/D2FO00350C
68. Xu D, Hu M-J, Wang Y-Q, Cui Y-L (2019) Antioxidant activities of quercetin and its complexes for medicinal application. Molecules 24:1123. https://doi.org/10.3390/molecules24061123
69. Sun X, Cameron RG, Bai J (2019) Microencapsulation and antimicrobial activity of carvacrol in a pectin-alginate matrix. Food Hydrocoll 92:69–73. https://doi.org/10.1016/j.foodhyd.2019.01.006
70. Rizfa MS, Yudiati E, Wijayanti DP (2020) Improving the antioxidant activity of sodium alginate from Sargassum sp. by thermal heating and chemical methods. J Kel Trop 23:284–290. https://doi.org/10.14710/jkt.v23i3.8946
71. Sellimi S, Younes I, Ayed HB, Maalej H, Montero V, Rinaudo M, Dahia M, Mechichi T, Hajji M, Nasri M (2015) Structural, physicochemical and antioxidant properties of sodium alginate isolated from a Tunisian brown seaweed. Int J Biol Macromol 72:1358–1367. https://doi.org/10.1016/j.ijbiomac.2014.10.016
72. Jakhar R, Paul S, Park YR, Han J, Kang SC (2014) 3,5,7,3′,4′-Pentamethoxyflavone, a quercetin derivative protects DNA from oxidative challenges: potential mechanism of action. J Photochem Photobiol, B 131:96–103. https://doi.org/10.1016/j.jphotobiol.2014.01.003
73. Chien W-J, Saputri DS, Lin H-Y (2022) Valorization of Taiwan's *Citrus depressa* Hayata peels as a source of nobiletin and tangeretin using simple ultrasonic-assisted extraction. Curr Res Food Sci 5:278–287. https://doi.org/10.1016/j.crfs.2022.01.013
74. Londoño-Londoño J, de Lima VR, Lara O, Gil A, Pasa TBC, Arango GJ, Pineda JRR (2010) Clean recovery of antioxidant flavonoids from citrus peel: optimizing an aqueous ultrasound-assisted extraction method. Food Chem 119:81–87. https://doi.org/10.1016/j.foodchem.2009.05.075
75. Shahrin EWE, Narudin NAH, Padmosoedarso KM, Kusrini E, Mahadi AH, Shahri NNM, Usman A (2021) Pectin derived from pomelo pith as a superior adsorbent to remove toxic acid blue 25 from aqueous solution. Carbohydr Polym Technol Appl 2:100116. https://doi.org/10.1016/j.carpta.2021.100116
76. Zamri NII, Zulmajdi SLN, Daud NZA, Mahadi AH, Kusrini E, Usman A (2021) Insight into the adsorption kinetics, mechanism, and thermodynamics of methylene blue from aqueous solution onto pectin-alginate-titania composite microparticles. SN Appl Sci 3:222. https://doi.org/10.1007/s42452-021-04245-9
77. Seida Y, Tokuyama H (2022) Hydrogel adsorbents for the removal of hazardous pollutants—requirements and available functions as adsorbent. Gels 8:220. https://doi.org/10.3390/gels8040220
78. Das KK, Reddy RC, Bagoji IB, Das S, Bagali S, Mullur L, Khodnapur JP, Biradar MS (2019) Primary concept of nickel toxicity–an overview. J Basic Clin Physiol Pharmacol 30:141–152. https://doi.org/10.1515/jbcpp-2017-0171
79. Mahey S, Kumar R, Sharma M, Kumar V, Bhardwaj R (2020) A critical review on toxicity of cobalt and its bioremediation strategies. SN Appl Sci 2:1279. https://doi.org/10.1007/s42452-020-3020-9
80. Leyssens L, Vinck B, Van Der Straeten C, Wuyts F, Maes L (2017) Cobalt toxicity in humans—a review of the potential sources and systemic health effects. Toxicology 387:43–56. https://doi.org/10.1016/j.tox.2017.05.015
81. Genchi G, Carocci A, Lauria G, Sinicropi MS, Catalano A (2020) Nickel: human health and environmental toxicology. IJERPH 17:679. https://doi.org/10.3390/ijerph17030679

82. Domingo JL (1989) Cobalt in the environment and its toxicological implications. In: Ware GW (ed) Reviews of environmental contamination and toxicology. Springer, New York, pp 105–132
83. Zhao L, Wang J, Zhang P, Gu Q, Gao C (2018) Absorption of heavy metal ions by alginate. In: Bioactive Seaweeds for Food Applications. Elsevier, pp 255–268
84. Gao X, Guo C, Hao J, Zhao Z, Long H, Li M (2020) Adsorption of heavy metal ions by sodium alginate based adsorbent-a review and new perspectives. Int J Biol Macromol 164:4423–4434. https://doi.org/10.1016/j.ijbiomac.2020.09.046
85. Abubakar Zauro S, Vishalakshi B (2018) Pectin graft copolymer-montmorillonite composite: synthesis, swelling and divalent metal ion adsorption. Sep Sci Technol 53:2170–2185.https://doi.org/10.1080/01496395.2018.1446987
86. Eliaz I, Weil E, Schwarzbach J, Wilk B (2019) Modified citrus pectin/alginate dietary supplement increased fecal excretion of uranium: a family. Altern Ther Health Med 25:20–24
87. Marangoni Júnior L, Fozzatti CR, Jamróz E, Vieira RP, Alves RMV (2022) Biopolymer-based films from sodium alginate and citrus pectin reinforced with SiO_2. Materials 15:3881. https://doi.org/10.3390/ma15113881
88. Singh P, Baisthakur P, Yemul OS (2020) Synthesis, characterization and application of crosslinked alginate as green packaging material. Heliyon 6:e03026. https://doi.org/10.1016/j.heliyon.2019.e03026

Publisher's Note